Automatic extraction of large-scale aquaculture encroachment areas using Canny Edge Otsu algorithm in Google Earth Engine – the case study of Kolleru Lake, South India

Abstract

The aquaculture expansion has made significant contributions to global food security, socio-economic development and, if implemented sustainably, can help preserve stable coastal environments. This study explicitly details the rapid expansion of large-scale aquaculture growth across the Kolleru and Upputeru regions of South India. We developed a novel classification method for automated extraction of aquaculture ponds in the Kolleru zone using the Canny Edge-Otsu algorithm to segment and extract the ponds applied to SAR-VV images in Google Earth Engine. This approach enables the area estimation of dense aquaculture ponds are essential for monitoring and management purposes. The results indicated that this method could effectively map the aquaculture ponds and the overall accuracy achieved in 2020 for the Kolleru and Upputeru areas by 90.6% and 95.7%, respectively. The aquaculture maps of this study can help government organizations, resource managers, stakeholders, and decision-makers understand the dynamics and plan sustainable measures in this area.

Keywords: Google Earth Engine, Canny Edge-Otsu threshold, Sentinel-1, Remote sensing, image segmentation

1. Introduction

Aquaculture farming is one of the important sources of food production, reinforced by global food security that almost raised five times between 1990 and 2015 (Ottinger et al., 2018). The projection of the human population by 2050 could reach up to 9.9 billion (PRB, 2020), resulting in a further increase in the demand for food, which might not be covered by agriculture and terrestrial livestock production alone. However, aquaculture has been one of the most promising sources of high-quality foods, covering increasing shares of the global food market over the last three decades (Porporato et al., 2020). Aquaculture has grown rapidly in coastal regions that are the most suitable conditions and occupy a significant number of coastal wetlands, introducing many impairments to the offshore environment (Xia et al., 2020). On the other side, it is causing detrimental effects such as pollution, ecological degradation, water eutrophication, and natural habitat destruction, mainly in coastal environments

(Kolli et al., 2020a; Sun et al., 2020; Nguyen et al., 2019; Peng et al., 2013). Nevertheless, the spatial planning of aquaculture management is essential for the sustainable growth of food to incorporate accurate mapping and monitoring of aquaculture (Gentry et al., 2016). However, spatial knowledge in the area of aquaculture distributions, patterns, and extent of aquaculture in coastal ecosystems is limited; therefore, it is essential to monitor those areas for food security and long-term environmental stability for sustainable management of the coastal regions. Satellite remote sensing takes advantage of both spatial and temporal data over decades is useful for the regional, continental, and global spatial scales providing tremendous economic benefits when used to observe changes on the ground (Pettorelli et al., 2014). Remote sensing data is useful for large-scale aquaculture mapping, monitoring, and quantitatively evaluating potential aquaculture distribution and dynamics with greater accuracy. Furthermore, satellite images provide reference maps for optimal planning and management of sustainable aquaculture in coastal environments (FAO, 2016).

Several studies have used satellite data to extract aquaculture ponds from small-scale to larger-scale regions (Sun et al., 2020; Stiller et al., 2019; Zhang et al., 2013; Alexandridis et al., 2008). The data sets used for aquaculture mapping range from high-resolution sensors with spatial resolutions of 5 m or finer (Prasad et al., 2019; Ottinger et al., 2017; Loberternos et al., 2016; Szuster et al., 2008) to coarser resolution, such as Landsat's optical sensors (Duan et al., 2020b; Wu et al., 2018; Pardo et al., 2012). The main disadvantage with optical datasets is that they cannot penetrate through the clouds, which have a negative impact on data quality, particularly in coastal regions where aquaculture ponds are prevalent. In comparison with optical sensors, the signal of radar imageries is polarized and operates longer wavelengths that can penetrate through clouds, vegetation, and soil, thus performing better for mapping aquaculture distribution (Fan et al., 2015).

A number of classification methods have been implemented to map aquaculture, although visual interpretation is the most appropriate method of mapping aquaculture ponds (Xu et al., 2014; Wen et al., 2011). The automated extraction of aquaculture ponds from remote sensing images is categorized into four types: (1) the classification approaches are used to determine the aquaculture from the separation of land and water features; for example, several studies have used supervised or unsupervised classification methods to distinguish aquaculture areas from other landuse classes (Fruhe et al., 2021; Proisy et al., 2018; Perez et al., 2003); (2) the edge detection method, is attributed to extract the boundaries of aquaculture ponds; (3) the band thresholding methods, which is one of the most significant approaches to extract aquaculture ponds, and based on spectral and textural attributes of an image. Many studies have developed automatic extraction models depending on the data source and classification methods to improve the mapping efficiency (Zhang et al., 2010). For example, Xia et al. (2020) proposed a multi-threshold segment method to extract aquaculture ponds based on the Random Forest classification model. Further, their results indicated that this approach could significantly improve the efficiency of extracting aquaculture ponds over larger areas. Li et al. (2017) proposed an adaptive threshold method for detecting uneaten fish food in underwater images, while Ottinger et al. (2017) developed a connected component segmentation algorithm to extract aquaculture ponds automatically; (4) the Object-Based detection analysis approach, which so far has mainly been used for delineating coastal aquaculture ponds accurately (Virdis, 2014; Du et al., 2013). Fu et al. (2019) proposed a method for extracting ponds by combining multi-scale segmentation and object-based neighbor features, demonstrating that this method performed better than other conventional methods.

Google Earth Engine (GEE) currently offers one of the most comprehensive and powerful platforms for this purpose, with access to more data and analysis. GEE was one of the first web-based platforms that enabled users to access the large volume of Earth Observation Analysis-Ready-Data (ARD) for rapid large-scale analytics (Gorelick et al., 2017). Many studies have taken advantage of GEE to map ground features ranging from small-scale to large-scale areas, particularly for visualizing, mapping, and modeling purposes (Duan et al., 2020a; Mutanga & Kumar, 2019). The aquaculture extraction studies based on GEE mostly used the spatial and spectral indices using a trial-and-error procedure or manual threshold detection followed by textural or morphological properties. This study developed a method for the automated extraction of aquaculture ponds using the Otsu threshold detection model and applied a Canny edge filter to extract the full extent of aquaculture in the Kolleru zone, an important prerequisite for aquaculture management in this area.

The previous studies conducted remote sensing and GIS techniques to analyze land use conditions and identify the fishponds extent areas in the Kolleru Lake (Pattanaik et al., 2010; Jayanthi et al., 2006; Rao et al., 2004). Further, few studies described the tremendous changes in Kolleru Lake because of the aquaculture encroachment by humans, followed by the government restoration activities that severely affected the lake ecosystem to an extent (Kolli et al., 2020a; Azeez et al., 2011). These studies analyzed the fishponds areas based on the land use classification maps using remote sensing methods up to a 3'ft contour interval. More than its lake area, the aquaculture development in the whole extent of Kolleru and its tributary Upputeru regions have explicitly shown tremendous aquaculture growth over the past three decades, drawing attention to the international literature due to scalability, massive distribution, and large-scale aquaculture production. This is the first study to map the intensive distribution of aquaculture ponds in this area, building on previous studies which analyzed the landuse conditions but limited to soil erosion, sediment pollution, shrinkage, and landuse changes. The methodological focus of this paper is utilizing the GEE platform to model the Kolleru zone abundance aquaculture to extract geometrical, topographical, and textural properties of aquaculture ponds from the Sentinel-1 SAR data using the Canny Edge-Otsu method to map their spatial distribution and variability. The results of this study are useful for understanding the Kolleru zone aquaculture for better planning and management for sustainable aquaculture growth in this region.

2. Study area

Kolleru Lake is one of the largest shallow freshwater lakes in India and is recognized to be of international importance under the Ramsar Convention. It is connected to the Bay of Bengal through a 60km long intricately meandering channel called "Upputeru River" (salt stream). It is located on the southeast coast of India, as shown in Figure 1. This region is well known for paddy cultivation and aquaculture farming. Geographically, the area is situated between 16º 19′ 10″ and 16º 47′ 33″ Northern latitude and 80º 56′ 22″ and 81º 37′ 42″ Eastern longitude. It is one of the highly promising coastal economic zones in India, approximately expanding over 1,120 km^2. Many rivers and irrigation canals flow through the lower part of the zone and, along with 68 minor irrigation channels, form large river deltas such as the Godavari River Delta and Krishna River Delta (which jointly form the Kolleru-Upputeru Catchment (Kolli et al., 2020a; Rao, 2003). The region's peculiar hydrography offers suitable conditions for large-scale aquaculture growth. The coastal region is, therefore, one of the economically most developed parts of Andhra Pradesh (India). Whereas, on the one hand, the growing demand for aquacultural products has benefited the regional economy, local stakeholders are at the same time becoming increasingly concerned about the environmental tradeoffs. They affect both the Kolleru and Upputeru aquaculture farmings, which are two distinct ecosystems, i.e., the freshwater system of Kolleru and the increasingly saline Upputeru system (Azeez et al., 2011). During extreme flood events, all of the Kolleru Lake region's bed villages are submerged underwater. On the other hand, the Upputeru, as its only outlet river, extends 61 km in length, connecting Kolleru Lake and the Bay of Bengal. During summers, the lake area completely dries up, whereas saltwater intrusion occurs due to the reverse flow of water through the Upputeru (i.e., Upputeru = salt stream), which leads to pollution (Acharyulu et al., 2019).

Aquaculture has been booming in Andhra Pradesh since the 1970s and has become one of the largest producers of farmed fish and shrimp in India (Belton et al., 2017). According to the 2018 statistical reports, Andhra Pradesh accounted for the highest inland and freshwater fish production. National Aeronautics and Space Administration (NASA) has released a recent abundance of large-scale aquaculture blueprints, which showed a dense area of inland aquaculture ponds along the Upputeru River in Andhra Pradesh, where people once raised crops (https://earthobservatory.nasa.gov/images/148581/an-abundance-of-aquaculture-in-andhra-pradesh). Aquaculture has replaced other land uses due to frequent flooding, as well as saltwater intrusion from the reverse flow of water into agricultural lands and the Bay of Bengal cyclones. Therefore, the state government made initial efforts to convert to aquaculture while also ensuring sustainable management of lake resources. Despite the fact that the successful growth of aquaculture in this region was a profitable choice for farmers, a critical expansion of aquaculture could be observed over the last three decades (Kolli et al., 2020a). As there is an increase in demand for fish production, farmers are encouraged to practice aquaculture, and the area is developed with small-scale industries for supporting aquaculture production. In our previous studies, we addressed the various factors that influence the lake through continuous land-use change conditions (Kolli et al., 2020a, Kolli et al., 2020b). The lake area is completely degraded by three important factors: the first reason is that non-point source pollution from agriculture in the upper catchment area causes eutrophication in the lake. Secondly, large-scale encroachment of aquaculture in the lake region leads to pollution, biodiversity loss, and massive weed infests. Thirdly, domestic and industrial sludge materials are directly discharged into the lake without treating the effluent materials.

3. Data sets and Methodology

This study used Sentinel-1 data from a dual-polarization composed of C-band Synthetic Aperture Radar (SAR) data for visualization and analysis purposes. The advantage of the SAR is where the data acquisition is available day and night conditions and penetrates through clouds and vegetation. This study aims to analyze the SAR data for a potential map of aquaculture ponds across the Kolleru and Upputeru regions. The SAR data was processed in Google Earth Engine (GEE) and further performed radiometric slope correction (Vollrath et al., 2020), speckle noise removal (Choi & Jeong, 2019), Otsu threshold detection applied on the Canny edge operation (Setiawan et al., 2017), is depicted in Figure 2. In the proposed method, radiometric slope correction and speckle noise is filtered first, and then permanent water classes are masked out from an image.

3.1. Speckle noise

Speckle noise is the most common phenomenon in SAR images, and it is caused by the reflection of the out-of-phase waves from a target. With the presence of speckle noise, it is difficult to interpret the image features, and further, it degrades the data quality for analysis (Huang et al., 2009). Therefore, in this study, the speckle filter analysis was performed on the Sentinel-1 images in GEE before the data was integrated for further analysis for mapping. In this process, all the similar pixels on an image are formed into a group of clusters. The nonlinear anisotropic diffusion method was applied to Sentinel-1 images in GEE to remove the speckle feature distractions (Perona & Malik, 1990) and enhance the quality of images.

3.2. Radiometric Slope Correction

Before the data is available onto the GEE platform, SAR ARD images are geometrically terrain-corrected, which includes noise reduction, radiometric correction, and geocoding. On the other hand, angular-based radiometric slope correction and transmission of invalid data masks over areas affected by shadow and layover are essential prior to perform analyses in GEE (Vollrath et al., 2020). Therefore, based on a simplified angular relationship between the SAR image and terrain geometry, this study performed Sentinel-1 based radiometric slope correction in GEE. The definitions and theoretical derivations are taken from the work by Hoekman & Reiche (2015).

The radar look direction is based on two angles: the incident (nominal) θ_i and the range (or look) direction ϕ_i. The incidence angle is derived as the angle formed by the normal and backscatter directions of the flat earth surface. In contrast, the range direction ($\phi_i = 90 - \theta$) is defined as the angle in the horizontal plane to the true north and significantly varies with latitude. Similar way terrain geometry is derived from the slope steepness ϕ_s and slope aspect angle α_s relative to true north, respectively. It can be modeled from a DEM with the same or better resolution than the image. In GEE, the slope steepness and aspect angle are directly calculated from the given DEM with the *ee.Terrain* class, respectively. We used a DEM derived from the SRTM and the Advanced Land Observing Satellite (ALOS), World 3D-DEM (AW3D) (Tadono et al., 2015) for analysis. The slope steepness in the range α_r and the slope aspect in azimuth α_{az} is inferred from the simplified relation between image and terrain geometry. The four angles are reduced to three by deducting the slope aspect angle of the terrain from the SAR range direction as follows:

$$\phi_r = \phi_i - \phi_s \quad (1)$$

The slope steepness angle as in range direction: α_r as determined by

$$tan(\alpha_r) = tan(\alpha_s)cos(\phi_r) \text{ or} \quad (2)$$
$$\alpha_r = arctan\big(tan(\alpha_s)cos(\phi_r)\big)$$

The slope aspect angle in azimuth direction: α_{az} which follows from

$$tan(\alpha_{az}) = tan(\alpha_s)\, sin(\phi_r) \quad \text{or} \quad (3)$$
$$\alpha_{az} = arctan\big(tan(\alpha_s)sin(\phi_r)\big)$$

The $\theta_\triangle$ is the local incident angle, which is derived from the angle between backscatter direction to a normal surface direction is follows:

$$cos(\theta_\triangle) = cos(\alpha_{az})\, cos(\theta_i - \alpha_r) \quad (4)$$

The final output of geocoded Sentinel-1 backscatter bands requires to be reconverted from the DB scale to its original format. Therefore, all the DB scale parameters are corrected to the normalized radar cross-section σ^0 as well as the incident angle also affects the radar backscatter values θ_i which is derived from the following equation:

$$\gamma^0 = \sigma^0 / cos(\theta_i) \quad (5)$$

Further, the relief modulation factor is defined as the ratio of backscatter coefficient on inclined terrain γ^0 to the backscatter on flatter terrain γ_f^0.

$$\gamma_f^0 = \gamma^0 \frac{tan(90 - \theta_i)}{\tan(90 - \theta_i + \alpha_r)} \quad (6)$$

Finally, the backscatter data is converted into a DB scale, and the corrected radiometric slope correction images were used for further analysis.

3.3. Canny Edge Otsu method

3.3.1 Canny Edge detection

The Canny operator is one of the most widely used edge detection algorithms to detect edges in images due to its superior performance (Rong et al., 2014). This study proposed the Canny edge detection method combined with Otsu thresholding to extract ponds. The Otsu algorithm optimizes Canny's dual-threshold and improves the edge detection performance (Cao et al., 2018). The initial threshold was chosen -18 based on our study's trial and error method after a number of average training samples evaluations in GEE. The initial threshold was used only to separate between water and non-water areas, whereas to get preliminary water samples. Further, the Canny edge detection operation was performed with the *ee.Algorithms.CannyEdgeDetector* in GEE, respectively (Fig. 3). Fig. 3a & 3b depicts an example of a result for each process in the Canny Edge detection method.

3.3.2 Otsu Thresholding

In image analysis, automatic and data-driven approaches with multispectral bands are always challenging to distinguish between two different types of relatively homogeneous features. However, a two-class segmentation can be performed for single-band images due to their bimodal pixel distribution to identify a threshold separating the two classes. The manual method of threshold selection using a trial-and-error procedure is complex and time-consuming; however, it would not be optimal. Nobuyuki Otsu (1979) developed an unsupervised nonparametric technique of automatic threshold selection based on observed distribution pixels (Eqn 7). The Otsu method can compute the optimum threshold value based on the maximization of the between-class variance in the foreground and background pixels in the image. The partition of the data maximizes inter-class variance is defined as follows:

$$BSS = \sum_{k=1}^{p}(\overline{DN}_k - \overline{DN})^2 \quad (7)$$

where, BSS is between-sum-of-square, and p is the number of defined classes (i.e., two classes defined in this study (0 = not-water, 1 = water), therefore p = 2). The Otsu function returns the mean value corresponding to the maximum BSS. DN is the digital number of the preferred band and $\overline{DN}_k$ indicates mean digital number in class k, and $\overline{DN}$ is the mean digital number of the entire dataset. The bins present the different selection of thresholds in a histogram generated in this study, as shown in Fig 3c. The automatic threshold was detected from the Canny Otsu method is -15.4, where this threshold is used to segment aquaculture ponds within the edge buffer zone. Figure 4 depicts as an example code for the integration of canny edge results with thresholding.

3.4. Training and validation datasets

We created two independent datasets and grouped all aquaculture ponds into one class and non-aquaculture ponds into another. A total of 172 test samples were collected from high-resolution Google Earth images, including 102 aquaculture polygons and 70 non-aquaculture polygons, respectively. The accuracy of the resulting aquaculture maps was assessed in comparison to a validation dataset. Aquaculture ponds are found near rivers, streams, and lakes, and they have a regular shape, darker colors, and are distributed in areas with a lot of water. Therefore, the aquaculture ponds are easy to distinguish from other water bodies when selecting the training polygons. The validation data set was generated using a stratified random sampling approach based on high-resolution images from Google Earth for the accuracy assessment. Further, the post-processing analysis was performed to extract the small streams and water bodies. During the classification, a small water body appears to be an aquaculture pond. Therefore, we used a water mask layer obtained from the Indian GeoPlatform portal to remove the permanent water bodies and small streams to enhance the classification results.

4. Results

4.1 Spatial dynamics of aquaculture ponds

This study developed the Canny Edge Otsu algorithm method based on GEE to automatically extract the aquaculture ponds in the Kolleru and Upputeru regions of Andhra Pradesh using Sentinel-1 images. The results provide a comprehensive overview of the spatial distribution of aquaculture ponds in the Kolleru flood basin zone (Fig. 5 & Fig. 6). In 2020, the total area of aquaculture ponds accounted for 1,176 km^2. The aquaculture area in the Kolleru wetland region was largest at 706.2 km^2, and the Upputeru River region was the smallest at 470 km^2, respectively.

Fig. 6 shows that aquacultures are densely occupied on both sides of the Upputeru river and distinguish a unique ecosystem and ecological balance in this region. This area is the fastest-growing aquaculture in India, and a series of embankments are identified in the Sentinel-1 image delineated by the Canny edge algorithm. The classification results showed that the aquaculture ponds that are widely distributed in the Kolleru area face pollution and ecological degradation problems. In contrast, the Upputeru catchment faces sea-level rise, saltwater intrusion, and reverse flow of water during flooding shifted the focus towards building aquaculture ponds for a stable environment.

Aquafarms are one of the most important land-use forms in this zone. We extracted the aquaculture ponds area of both Kolleru and Upputeru from 2015 to 2020 (see Fig. 7). The aquaculture ponds occupied in the Kolleru wetland area are larger than that of the Upputeru region. The results show that the extraction of aquaculture area in Kolleru in 2015 was 630.7 km^2, which increased to 642.5 km^2 by 2016. Further, a reduction of 12.4 km^2 of the area was observed in 2017 due to the area used for nontraditional aquaculture methods, including paddy cultivation, vegetation, and weed infests. In 2018, the aquaculture area occupied was 690.8 km^2 and increased to 706.2 km^2 in 2020, respectively. In contrast, in Upputeru, the aquaculture area is increased from 415 km^2 to 470 km^2, indicating that the region is continuously expanding the aquaculture to meet the state government's demands of food security goals.

4.2 Accuracy assessments of the classification map

To assess the accuracy based on validation data sets, a standard accuracy test was performed in the Kolleru and Upputeru regions. However, 80% of the data was used to train the model, whereas 20% of the data was used to validate based on a confusion matrix. The statistics of accuracy, including producer's accuracy, user's accuracy, overall accuracy, and Kappa coefficient, were obtained from 2020 classification results are summarized in Table 1. The results indicated that the extraction of aquaculture ponds had a high accuracy of 92.6% for the Kolleru area, with a Kappa coefficient of 0.91. For the Upputeru area, a very high accuracy of 95.7% was achieved, and the Kappa coefficient was 0.94, respectively. The classification error was occurred for the Kolleru area because of the similarity of the pixel values between aquaculture and lake. It is difficult to interpret the area with water characteristics and similar way with small aquaculture ponds.

To further evaluate the accuracy of our method, we performed a comparative study analysis for visually interpreting the aquaculture ponds using very high-resolution images were acquired from Google Earth to visualize the results. Fig 8 depicts our classification results for 2020 from the automated extraction of fishponds based on the Otsu threshold method is identical to that same visual interpretation results. The proportion of the aquaculture area of the Google Earth image and Sentinel-1 area overlaps with the Canny edge boundary for better visualization. The classification results show that the Edge Otsu threshold method can accurately extract the aquaculture ponds from the Sentinel-1 images. However, the proportions of the aquaculture area from automatic extraction and landuse classification method of the overlapping areas in the Kolleru area are 95% and 92%, whereas in the Upputeru area are 94% and 90%, respectively (Table 2).

5. Discussion

Many studies have been conducted to extract aquaculture ponds using remote sensing satellite images (Ottinger et al., 2017; Fan et al., 2015). The most significant approach using Sentinel-1 images is fully automated, has a high spatial resolution and longer wavelength that can distinguish the properties under the vegetation. However, SAR-VV polarization is ideal for the study of aquaculture ponds due to the signal’s penetration through the canopy and its ability to sense if there is standing water under the vegetation and better identify the spectral and textural characteristics of an image. Our study performed the automatic extraction method on SAR images for aquaculture mapping in the Kolleru zone. The Otsu method of determining the optimal threshold for detecting the aquaculture pixels based on the Canny edge operator achieved high accuracy. This method can be adopted for dense inland aquaculture mapping in large areas. Several studies focused on extracting massive distribution of aquaculture ponds from adjacent rivers, lakes, and wetlands (Ottinger et al., 2017; Ma et al., 2010). The separation of individual aquaculture ponds is difficult while excluding the dikes between them. Duan et al. (2020a) considered the aquaculture region to be relatively consistent with aquaculture land use parameters and developed a method to extract ponds by integrating spectral, spatial, and morphological features. At the same time, if it is related to the missing out or aggregated small ponds, the effectiveness of these studies is limited. The application of relevant indices includes water index, texture, and geometric metrics derived from radar backscatter to segment or extract aquaculture ponds, significantly improving the classification results (Sun et al., 2020). On the other hand, Wang et al. (2020) proposed a pixel-and phenology-based algorithm to map coastal wetlands at large scales. The results demonstrated that the study achieved a very high accuracy of 98% using the pixel-based method.

The image segmentation method is another approach to map inundated areas and uses object-based features (OBF) to distinguish between aquaculture and non-aquaculture ponds (Yu et al., 2020). The aquaculture pond area is a stagnated water body is divided by the roads and dikes. It is difficult to distinguish the background of the ponds with the presence of other spectral features by threshold and water index. However, recent studies have developed an automatic extraction of aquaculture ponds using threshold selection, machine learning models, and object-based methodologies to improve pond mapping accuracy (Duan et al., 2020b; Wu et al., 2018). The threshold selection is a group of pixels with a similar value that adjusts to extract ponds. For example, Xia et al. (2020) demonstrated that automatic extraction of aquaculture ponds could be achieved through the multi-threshold connected component segmentation and random forest classification model. This method is highly recommended for the non-intensive aquaculture ponds, and they achieved an overall accuracy of 91.8%. Our study focused on the edge detection operator for automatically extracting aquaculture ponds using the Canny Edge Otsu threshold method. The main objective was not only to extract the massive aquaculture ponds but also to delineate the small size ponds accurately.

Google was among the first to enable the shift towards using EO big data cloud platforms when it introduced the Google Earth Engine (GEE) in 2010 to enhance the use of satellite imagery for large-scale and time series applications. All data source available on GEE has its own time series of EO/ARD data organized into a stack called Image Collection. The integration of earth observation data into GEE platforms for potential use in land monitoring, detecting changes in global forests, precision agriculture analysis for economic development policies (Hansen et al., 2013). This framework is applicable for aquaculture monitoring using GEE to extract the information.

5.1. Limitations

This study attempts to comprehensively analyze SAR data pre-processed in Google Earth Engine for the aquaculture mapping. The analysis of the data is somewhat limited due to its geographic location and temporal variability. However, the aquaculture in the study area is largely distributed in a particular zone and clustered around the lake, and uniformly distributed along the Upputeru river, where the results might change for other areas of the world in difficult terrains and mountain regions. In flooded forested areas, where the C-band SAR signal cannot penetrate the canopy structure to view the underlying water, aquaculture mapping methods may have higher errors, and L-band SAR data is preferred. The SAR data is available from recent years, and it is difficult to compare with time-series analysis. There is a prominent trade-off between the spatial and temporal resolution of a single sensor as well as high resolution, and high revisiting frequency cannot be achieved by the same sensor. The possible solutions for obtaining the different spatial and temporal resolutions to generate aquaculture maps are based on the data fusion and data assimilation models from optical data sets such as Sentinel-2 and Landsat series. Therefore, merging the high spatial resolution and high temporal resolution of different sensors is an effective solution to generate aquaculture maps, but it is also involved in comprehensive data pre-processing analysis.

6. Conclusions

In this study, we proposed a new framework for automatically extracting the aquaculture ponds in the Kolleru and Upputeru areas based on the GEE platform. The radiometric correction and speckle noise filter were applied to the Sentinel-1 images for better visualization purposes. Through this method, we mapped the intense distribution, areas, and shape of Kolleru and Upputeru aquaculture ponds in 2020. We present the first assessment of the spatiotemporal dynamics of aquaculture pond areas based on earth remote sensing data for both the Kolleru and Upputeru areas. Overall, the results indicated that the proposed method achieved very high accuracy and further verified the classification results based on high-resolution from Google Earth images. This method has great potential to apply intense distribution of aquaculture ponds, wetland regions and manage coastal ecosystems. GEE set a benchmark in enabling universal access to its high-power cloud computing resources for fast retrieving and processing time series ARD from diverse sensors. The efficient use of GEE for mapping aquaculture from small-scale to large regions for visualization, mapping, analyzing, and modeling purposes. The use of these integrated tools allows up-to-date aquaculture monitoring.

Conflicts of Interest

The authors declare that they have no known competing financial interests or personal relationships that could have appeared to influence the work reported in this paper.

Data availability statement

Sources of all the data have been described properly. Derived data supporting the findings of this study are available from the corresponding author on request.

References:

Acharyulu, P.S.N.; Gireesh, B.; Venkateswarlu, Ch.; Apparao, A.P.V.; Prasad, KVSR (2019). The circulation and flow regime of Upputeru, outlet channels of Kolleru Lake, India. International Journal of Lakes and Rivers, 12, pp: 53-65.

Alexandridis, T.K.; Topaloglou, C.A.; Lazaridou, E.; Zalidis, G.C. (2008). The performance of satellite images in mapping aquacultures. Ocean Coast. Manag, 51, 638-644.

Azeez, PA; Kumar, A.; Choudhury, B.C.; Sastry, V.N.K.; Upadhyay, S.; Reddy, K.M.; Rao, K.K. (2011). Report on the Proposal for Downsizing the Kolleru Wildlife Sanctuary (+5 to +3 Feet Contour); The Ministry of Environment and Forests Government of India: New Delhi, India, 2011.

Belton, B.; Padiyar, A.; Ravibabu, G.; Rao, G.K. (2017). Boom and bust in Andhra Pradesh: Development and transformation in India's domestic aquaculture value chain. Aquaculture, 470, pp:196-206.

Cao, J.; Chen, L.; Wang, M.; Tian, Y. (2018). Implementing a parallel image edge detection algorithm based on the Otsu-Canny operator on the Hadoop Platform. https://doi.org/10.1155/2018/3598284.

Choi, H.; Jeong, J. (2019). Speckle noise reduction technique for SAR images using statistical characteristics of speckle noise and discrete wavelet transform. Remote Sensing, 11, 1184.

Duan, Y.; Li, X.; Zhang, L.; Chen, D.; Liu, S.; Ji, H. (2020a). Mapping national-scale aquaculture ponds based on the Google Earth Engine in the Chinese coastal zone. Aquaculture, 520, 734666.

Duan, Y.; Li, X.; Zhang, L.; Liu, W.; Liu, S.; Chen, D.; Ji, H. (2020b). Detecting spatiotemporal changes of large-scale aquaculture ponds regions over 1988-2018 in Jiangsu Province, China using Google Earth Engine. Ocean & Coastal Management, 188, 105144.

Du, Y.; Wu, D.; Liang, F.; Li, C. (2013). Integration of case-based reasoning and object-based image classification to classify SPOT images: a case study of aquaculture land use mapping in coastal areas of Guangdong province, China. GIScience & Remote Sensing, 50, 574-589.

Fan, J.; Chu, J.; Geng, J.;Zhang, F. (2015). Floating raft aquaculture information automatic extraction based on high-resolution SAR images. 2015 IEEE International Geoscience and Remote Sensing Symposium (IGARSS), pp: 3989-3901.

FAO. (2016). The state of world fisheries and aquaculture in 2016. Contributing to food security and nutrition for all. Rome.

Fruhe, L.; Cordier, T.; Dully, V.; Breiner, H.W.; Lentendu, G.; Pawlowski, J.; Martins, C.; Wilding, T.A.; Stoeck, T. (2021). Supervised machine learning is superior to indicator value inference in monitoring the environmental impacts of salmon aquaculture using eDNA metabarcodes. Molecular Ecology, 30, 2988-3006.

Fu, Y.; Deng, J.; Ye, Z.; Gan, M.; Wang, K.; Wu, J.; Yang, W.; Xiao, G. (2019). Coastal Aquaculture Mapping from Very High Spatial Resolution Imagery by Combining Object-Based Neighbor Features. Sustainability 2019, 11, 637.

Gentry, R.R.; Lester, S.E.; Kappel, C.V.; White, C.; Bell, TW; Stevens, J.; Gaines, S.D. (2016). Offshore aquaculture: Spatial planning principles for sustainable development. Ecology and Evolution, 7, pp:733-743.

Gorelick, N.; Hancher, M.; Dixon, M.; Ilyushchenko, S.; Thau, D.; Moore, R. (2017). Google Earth Engine: Planetary-scale geospatial analysis for everyone. Remote Sensing of Environment, 202, pp: 18-27.

Hansen, M.C.; Potapov, P.V.; Moore, R.; Hancher, M.; Turubanova, S.A.; Tyukavina, A.; Thau, D.; Stehman, S.V.; Goetz, S.J.; Loveland, T.R.; Kommareddy, A.; Egorov, A.; Chini, L.; Justice, C.O.; Townshend, J.R.G. (2013). High-resolution global maps of 21-st century forest cover change. Science 342 (6160), 850-853.

Hoekman, DH; Reiche, J. (2015). Multi-model radiometric slope correction of SAR images of complex terrain using a two-stage semi-empirical approach. Remote Sensing of Environment, 156, pp:1-10.

Huang, S.; Liu, D.; Gao, G.; Guo, Xi. (2009). A novel method for speckle noise reduction and ship target detection in SAR images. Pattern Recognition, 42, pp: 1533-1542.

Jayanthi, M.; Rekha, P.N.; Kavitha, N.; Ravichandran, P. (2006). Assessment of impact of aquaculture on Kolleru Lake (India) using remote sensing and Geographical Information System. Aquac. Res, 37, 1617–1626.

Kolli, M.K.; Opp, C.; Karthe, D.; Groll, M. (2020a). Mapping of Major Land-Use Changes in the Kolleru Lake Freshwater Ecosystem by Using Landsat Satellite Images in Google Earth Engine. *Water* 2020, *12*, 2493. https://doi.org/10.3390/w12092493.

Kolli, M.K.; Opp, C.; Groll, M. (2020b). Identification of critical diffuse pollution sources in an ungaguged catchment by using the SWAT model – A case study of Kolleru Lake, East Coast of India. AJGR 2020, 3, 53-68.

Li, D.; Xu, L.; Liu, H. (2017). Detection of uneaten fish food pellets in underwater images for aquaculture. Aquacultural Engineering, 78, 85-94.

Loberternos, R.A.; Porpetcho, W.P.; Graciosa, J.C.A.; Violanda, R.R.; Diola, A.G.; Dy, D.T.; Otadoy, R.E.S. (2016). An object-based workflow developed to extract aquaculture ponds from airborne LIDAR data: a test case in the central Visayas, Philippines. ISPRS- Int. Arch. Photogram. Remote Sens. Spatial Inf. Sci., XLI-B8, 1147-1152.

Ma, Y., Zhao, D., Wang, R., Su, W. (2010). Offshore aquatic farming areas extraction methods based on ASTER data. Transactions of the Chinese Society of Agricultural Engineering 26, 120-124.

Mutanga, O.; Kumar, L. (2019). Google Earth Engine Applications. Remote Sensing, 11(5), 591.

Nguyen, T.T.N.; Nemery, J.; Gratiot, N.; Strady, E.; Tran, V.Q.; Nguyen, A.T.; Aime, J.; Peyne, A. (2019). Nutrient dynamics and eutrophication assessment in the tropical river system of Saigon—Dongnai (southern Vietnam). Sci. Total Environ, 653, 370–383.

Otsu, N. (1979). A threshold selection method from gray-level histograms. IEEE Transactions on Systems, Man, and Cybernetics, 9(1), 62-66.

Ottinger, M.; Clauss, K.; Kuenzer, C. (2017). Large-scale assessment of coastal aquaculture ponds with Sentinel-1 time-series data. Remote Sens, 9, 440.

Ottinger, M.; Clauss, K.; Kuenzer, C. (2018). Opportunities and challenges for the estimation of aquaculture production based on earth observation data. Remote Sens. 2018, 10(7), 1076.

Pardo-Pascual, J.E.; Almonacid-Caballer, J.; Ruiz, L.A.; Palomar-Vazquez, J. (2012). Automatic extraction of shorleliens from Landsat TM and ETM+ multi-temporal images with subpizel precision. Remote Sens. Environ, 123, 1-11.

Pattanaik, C.; Prasad, S.N.; Nagabhatla, N.; Sellamuthu, S.S. (2010). A case study of Kolleru Wetland (Ramsar site), India using remote sensing and GIS. IUP J. Earth Sci, 4, 70–77.

Peng, Y.; Chen, G.; Li, S.; Liu, Y.; Pernetta, J.C. Use of degraded coastal wetland in an integrated mangrove–aquaculture system: A case study from the South China Sea. Ocean Coast. Manag. 2013, 85, 209–213.

Perez, F.A.; Luna, A.R.; Turner, J.; Robles, C.A.B.; Jacob, G.M. (2003). Land cover changes and impact of shrimp aquaculture on the landscape in the Ceuta coastal lagoon system, Sinaloa, Mexico. Ocean & Coastal Management, 46, 583-600.

Perona, P.; Malik, J. (1990). Scale-space and edge detection using anisotropic diffusion, IEEE Trans. Pattern Anal. Mach. Intell., Vol. 12, 629-639, 1990.

Pettorelli, N.; Laurance, W.F.; O'Brien, T.G.; Wegmann, M.; Nagendra, H.; Turner, W. (2014). Satellite remote sensing for applied ecologists: opportunities and challenges. Journal of Applied Ecology, 51, pp:839-848.

Population Reference Bureau (2020). http://sdg.iisd.org/news/world-population-to-reach-9-9-billion-by-2050/.

Porporato, E.M.D.; Pastres, R.; Brigolin, D. (2020). Site Suitability for Finfish Marine Aquaculture in the Central Mediterranean Sea. Front. Mar. Sci. 2020, 6, 772.

Prasad, K.; Ottinger, M.; Wei, C.; Leinenkugel, P. (2019). Assessment of coastal aquaculture for India from Sentinel-1 SAR time series. Remote Sens, 11, 357.

Proisy, C.; Viennois, G.; Sidik, F.; Andayani, A.; Enright, J.A.; Guitet, S.; Gusmawati, N.; Lemonnier, H.; Muthusankar, G.; Olagoke, A.; Prosperi, J.; Rahmania, R.; Ricout, A.; Soulard, B.; Suhardjono. (2018). Monitoring mangrove forests after aquaculture abandonment using time series of very high spatial resolution satellite images: A case study from the Perancak estuary, Bali, Indonesia. Marine Pollution Bulletin, 131, 61-71.

Rao, A. (2003). Polycyclic Aromatic Hydrocarbons in Sediments from Kolleru Wetland in India. Bull. Environ. Contam. Toxicol. 2003, 70, 964–971.

Rao, K.N.; Krishna, G.M.; Malini, B. (2004). Kolleru lake is vanishing—A revelation through digital image processing of IRS-1D LISS III sensor data. Curr. Sci, 86, 1312–1316.

Rong, W.; Li, Z.; Zhang, W.; Sun, L. (2014). "An improved Canny edge detection algorithm," 2014 IEEE International Conference on Mechatronics and Automation, pp: 577-582.

Sun, Z.;Luo, J.; Yang, J.; Yu, Q.; Zhang, L.; Xue, K.; Lu, L. (2020). National-scale mapping of coastal aquaculture ponds with Sentinel-1 SAR data using Google Earth Engine, Remote Sens, 12, 3086. https://doi.org/10.3390/rs12183086.

Setiawan, BD.; Rusydi, A.N.; Praditya, K. (2017). Lake edge detection using Canny Algorithm and Otsu Thresholding. International Symposium on Geoinformatics, 24-25 Nov. 2017. https://doi.org/10.1109/ISYG.2017.8280676.

Stiller, D.; Ottinger, M.; Leinenkugel, P. (2019). Spatio-Temporal patterns of coastal aquaculture derived from Sentinel-1 time series data and the full Landsat archive, Remote Sens, 11, 1707.

Szuster, B.W.; Steckler, C.; Kullavanijaya, B. (2008). Detecting and managing coastal fisheries and aquaculture gear using satellite radar imagery. Coast. Manag, 36, 318-329.

Tadono, T.; Takaku, J.; Tsutsui, K.; Oda, F.; Nagai, H. Status of “ALOS World 3D (AW3D)” global DSM generation. In Proceedings of the 2015 IEEE International Geoscience and Remote Sensing Symposium (IGARSS), Milan, Italy, 26–31 July 2015; pp. 3822–3825.

Virdis, S.G.P. (2014). An object-based image analysis approach for aquaculture ponds precise mapping and monitoring: a case study of Tam Giang-Cau Hai Lagoon, Vietnam. Environ Monit Assess 186, 117-133.

Vollrath, A.; Mullissa, A.; Reiche, J. (2020). Angular-based radiometric slope correction for Sentinel-1 on Google Earth Engine. Remote Sens, 12, 1867.

Wen, Q.; Zhang, Z.; Xu, J.; Zuo, L.; Wang, X.; Liu, B.; Zhao, X.; Yi, L. (2011). Spatial and temporal change of wetlands in Bohai rim during 2000-2008: an analysis based on satellite images. J. Remote Sens.; 15, pp:183-200.

Wu, Y.; Chen, F.; Ma, Y.; Liu, J.; Li, X. (2018). Research on automatic extraction method of coastal aquaculture area using Landsat8 data. Remote Sens. Land Resour. Pp: 96-105.

Xia, Z.; Guo, X.; Chen, R. (2020). Automatic extraction of aquaculture ponds based on Google Earth Engine. Ocean and Coastal Management, 198, 105348. https://doi.org/10.1016/j.ocecoaman.2020.105348.

Xu, Y.; Zhang, X.; Wang, X.; Wen, Q.; Liu, F.; Li, N. (2014). Remote sensing monitoring and temporal variation analysis of coastal aquaculture in Shandong province in the recent three decades. J. Geo-Inf. Sci., 16, pp: 482-489.

Zhang, T.; Yang, X.; Hu, S.; Su, F. (2013). Extraction of coastline in aquaculture coast from multispectral remote sensing images: Object-based region growing integrating edge detection. Remote Sens, 5, 4470-4487.

Zhang, T.; Li, Q.; Yang, X.; Zhou, C.; Su, F. (2010). Automatic mapping aquaculture in the coastal zone from TM imagery with OBIA approach. 2010 18th international conference on Geoinformatics, pp: 1-4.

Wang, X.; Xiao, X.; Zou, Z.; Hou, L.; Qin, Y.; Dong, J.; Doughty, R.B.; Chen, B.; Zhang, X.; Chen, Y.; Ma, J.; Zhao, B.; Li, B. (2020). Mapping coastal wetlands of China using time-series Landsat images in 2018 and Google Earth Engine. ISPRS Journal of Photogrammetry and Remote Sensing, 163, pp: 312-326.

Yu, Z.; Di, L.; Rahman, M.S.; Tang, J. (2020). Fishpond Mapping by Spectral and Spatial-Based Filtering on Google Earth Engine: A Case Study in Singra Upazila of Bangladesh. Remote Sens. 2020, 12, 2692. https://doi.org/10.3390/rs12172692.

Table 1. Accuracy assessment test for aquaculture and non-aquaculture classes. Producers accuracy, users accuracy, overall accuracy, and Kappa coefficient.

	Region	Aquaculture	Non-Aquaculture	Producer accuracy (%)	Users accuracy (%)	Overall accuracy (%)	Kappa
Aquaculture	Kolleru	647	62	94.1	87.9	90.6%	0.91
Non-Aquaculture		78	621	91.3	93.6		
Aquaculture	Upputeru	756	73	97.2	90.4	95.7%	0.94
Non-Aquaculture		91	694	89.6	93.1		

Table 2. A comparison of the results between visual interpretation and automated extraction in Kolleru and Upputeru areas.

	Visual interpretation (km^2)	Automated extraction		Lulc aquaculture proportion (km^2)	
		area (km^2)	proportion of the area	area (km^2)	proportion of the area
Kolleru Lake	741.79	706.2	0.95	687.2	0.92
Upputeru Region	495.7	470	0.94	448.5	0.90

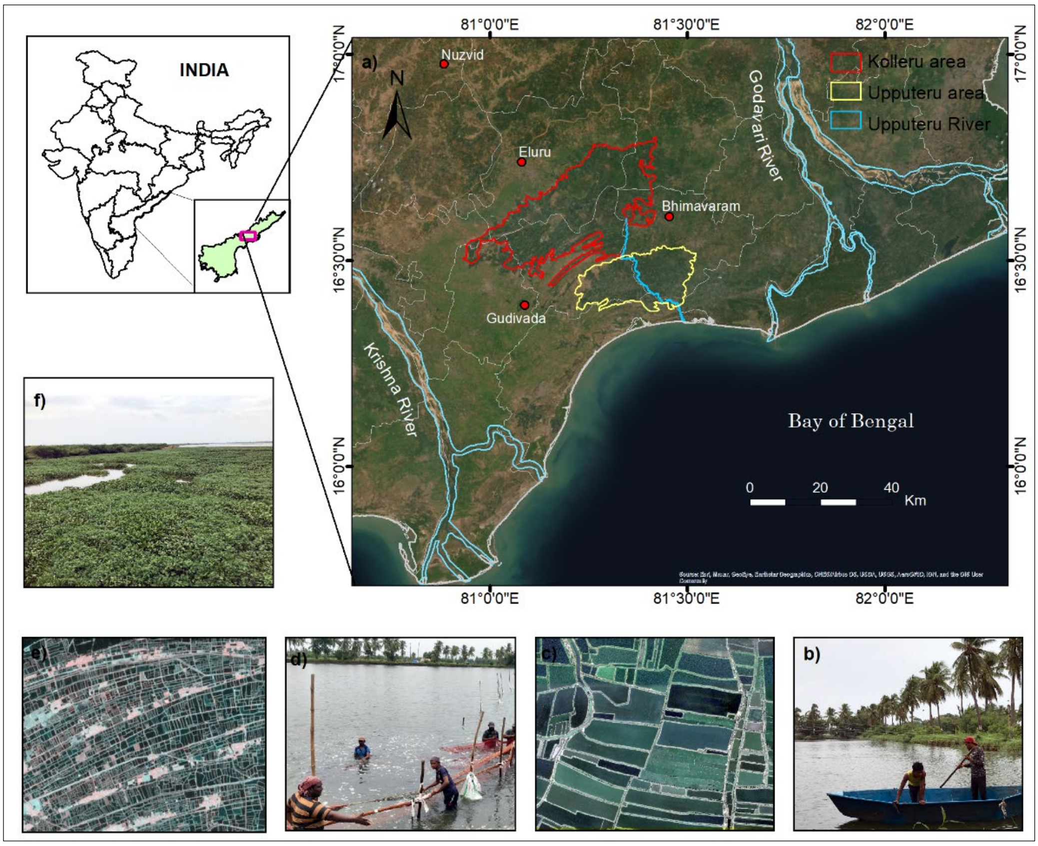

Figure 1. The location and overview of the study area: (**a**) Kolleru & Upputeru aquaculture regions (**b**) Aquaculture practicing (**c**) Freshwater ponds in Kolleru region (**d**) aquaculture harvesting (e) Salt fields in Upputeru region, and **f**) coverage of aquatic weeds [image b, d, and f: (Photo by, Monika Mandal, Sep 20, 2021)]

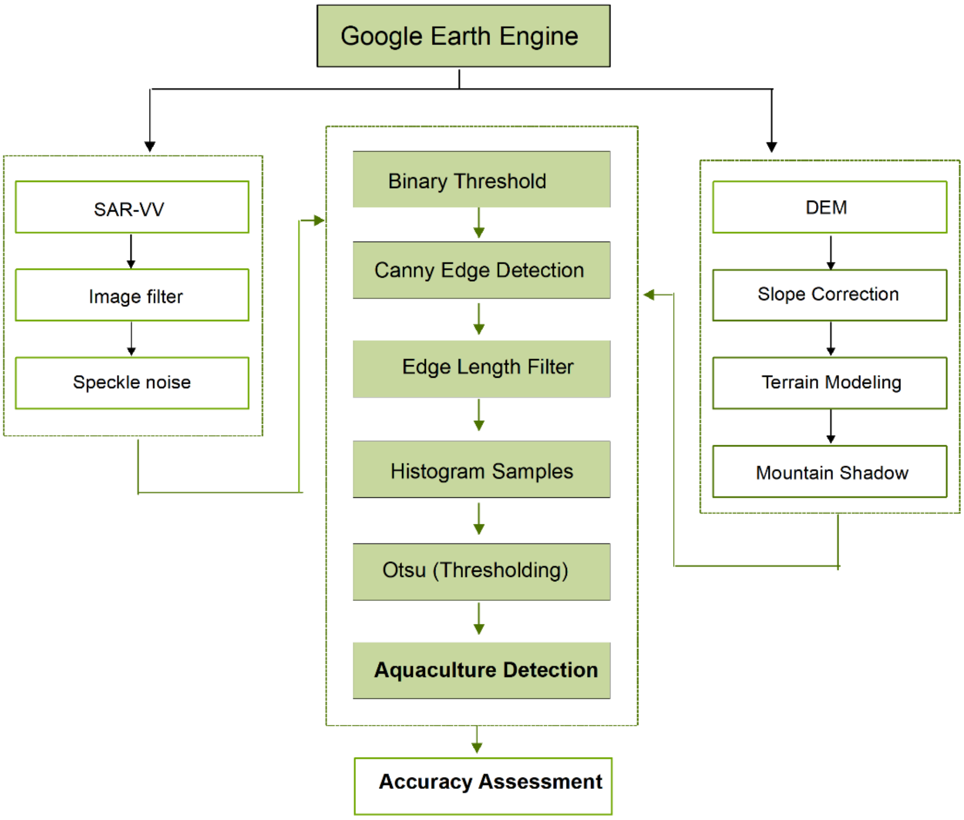

Figure 2. Methodology flowchart adopted in this study.

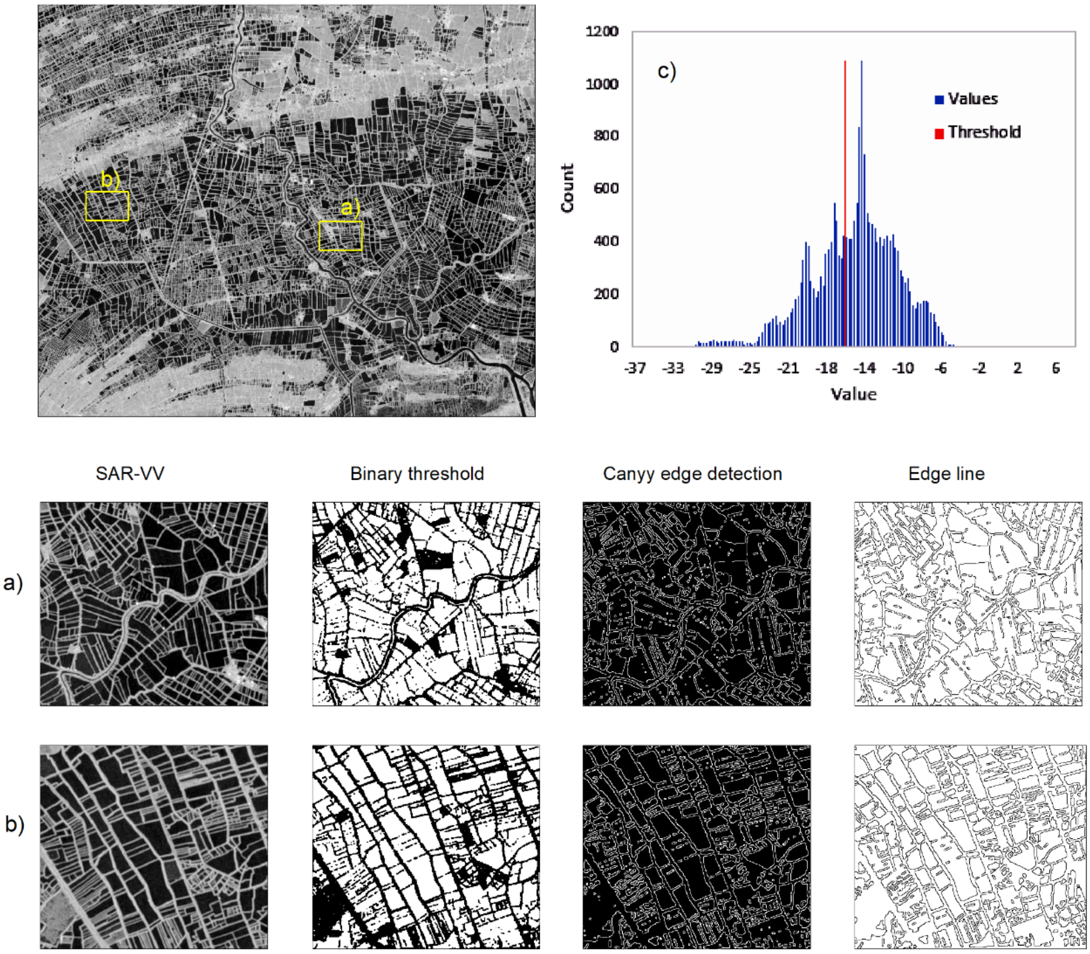

Figure 3. Detection of aquaculture ponds using Edge Otsu Algorithm in Upputeru region: a) Middle-Upputeru River, b) a recent encroachment of aquaculture, and c) Otsu threshold histogram

```
//canny edges
 var join  = canny.updateMask(canny).lt(cannyLt).connectedPixelCount(connectedPixels, true);
 segments      = join.gte(edgeLength);
 segments          = segments.updateMask(segments);
 Map.addLayer(segments,{},"segments")
  segmentsBuffer = segments.focal_max(smoothsegments, 'square', 'meters');
 Map.addLayer(segmentsBuffer,{},"segments buffer")
 // canny results integration with Otsu
 var histogram_imag = img.updateMask(segmentsBuffer);
 var histogram = ee.Dictionary(histogram_imag.reduceRegion({
   reducer:ee.Reducer.histogram(maxBuckets, minBucketWidth,maxRaw)
     .combine('mean', null, true).combine('variance', null,true),
   geometry: aquaculture,
   scale: reductionScale,
   maxPixels: 1e13,
   tileScale:16
 }).get(bandName.cat('_histogram')));
 var threshold = otsu(histogram);
```

Figure 4. Example code for integration of canny edge results with thresholding.

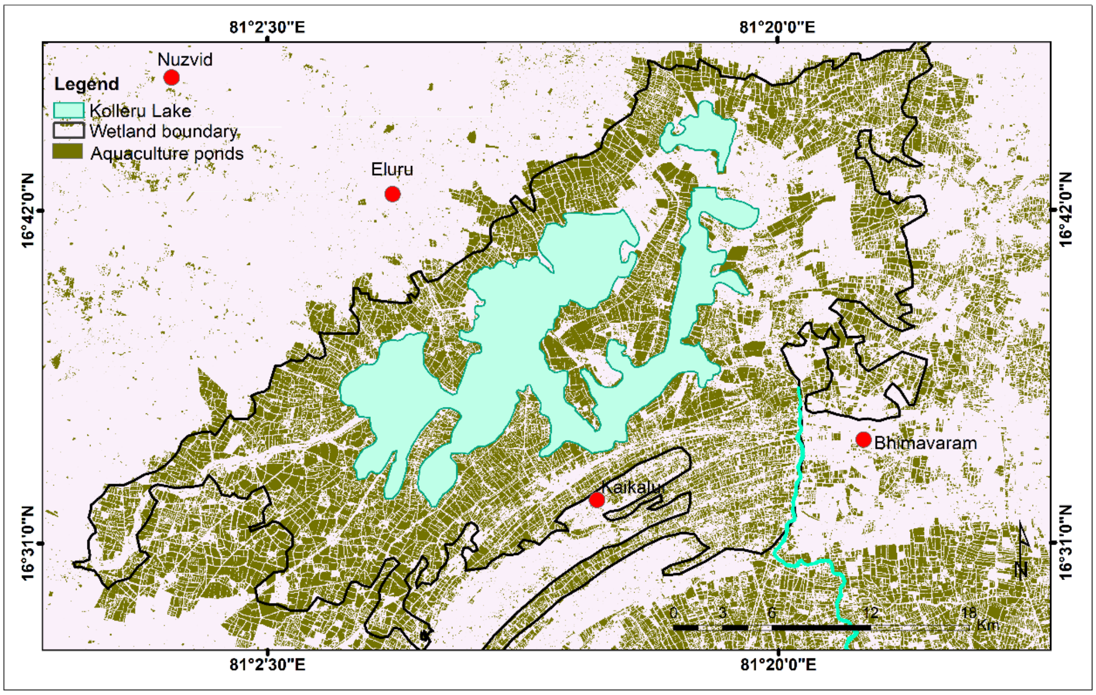

Figure 5. Spatial distribution of aquaculture ponds in the Kolleru Lake region in 2020

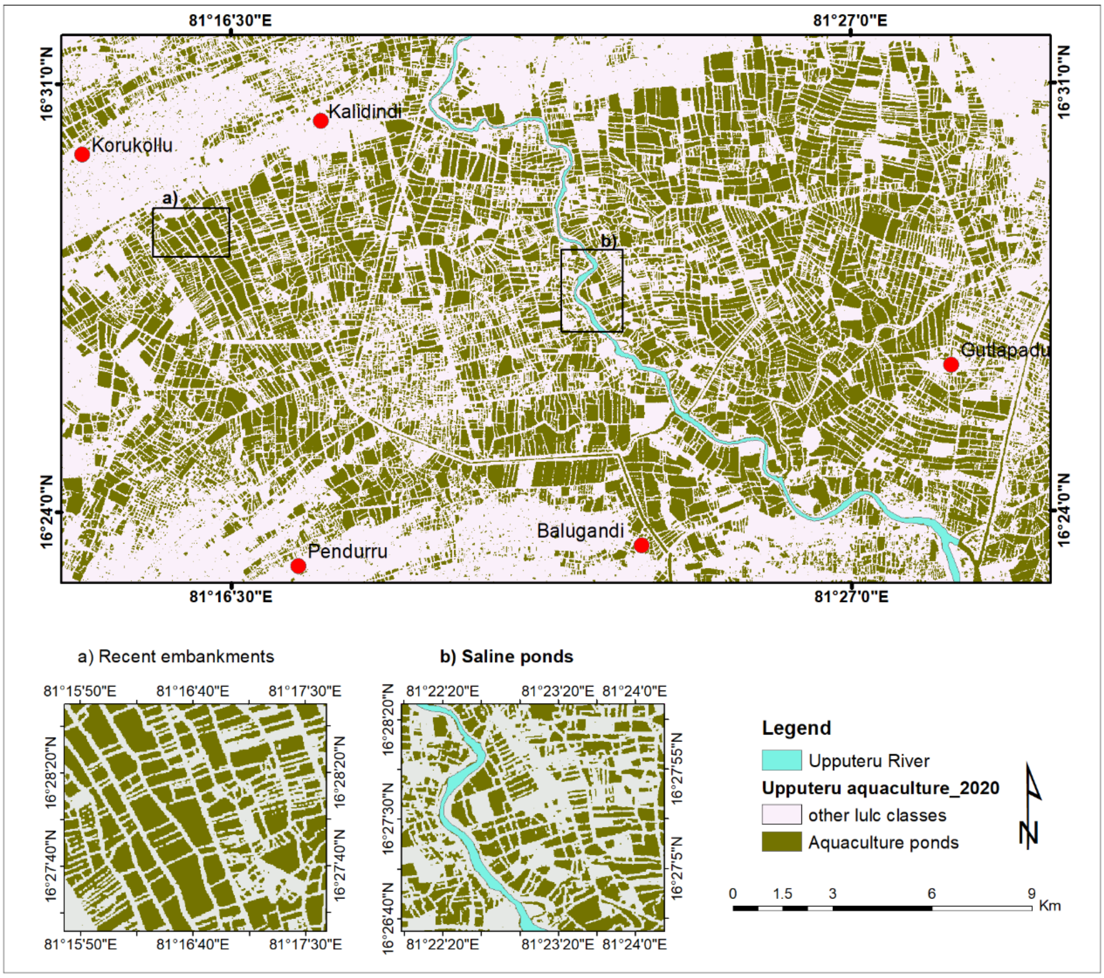

Figure 6. Spatial distribution of aquaculture ponds within the Upputeru River region in 2020 a) and b) shows the example of classification results of aquaculture ponds

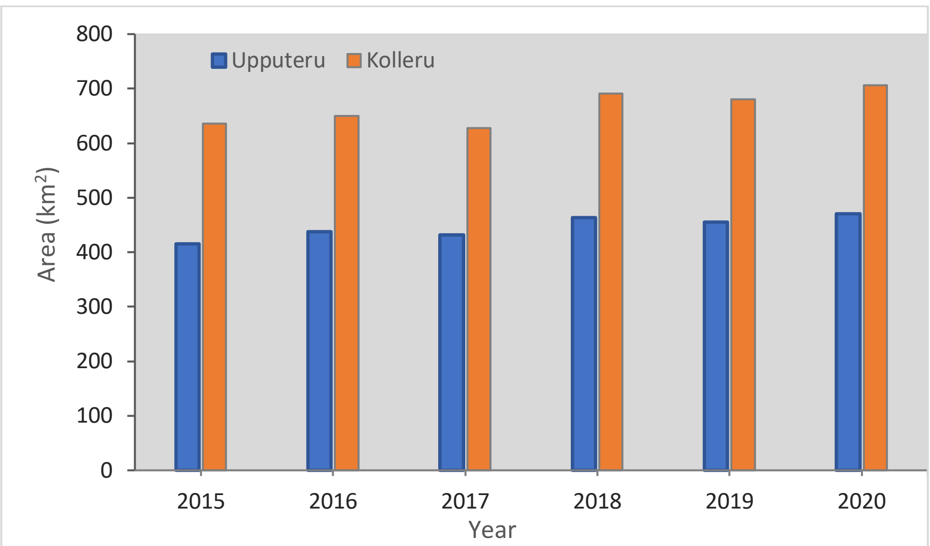

Figure 7. Areawise comparison of aquaculture ponds in Upputeru and Kolleru regions from 2015 to 2020.

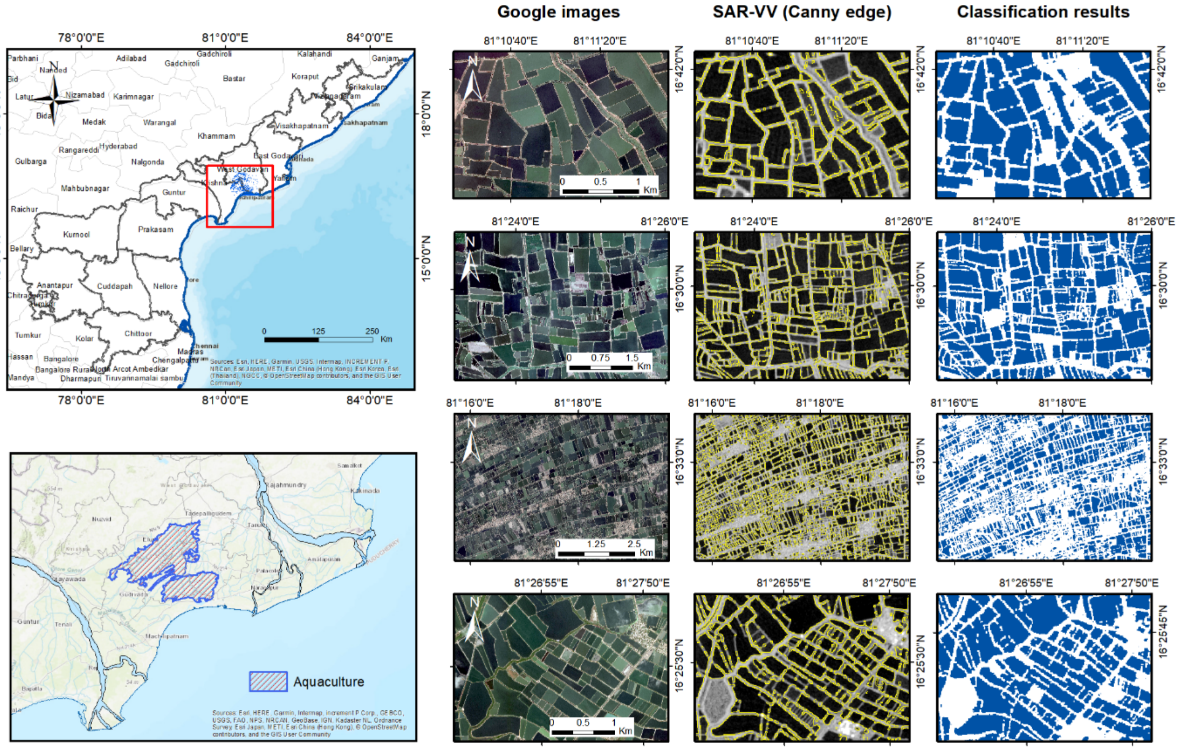

Figure 8. Extraction results of aquaculture ponds in 2020.